Adaptive fractional order sliding mode control for Boost converter in the Battery/Supercapacitor HESS

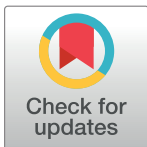Jianlin Wang[1,2], Dan Xu[1]*, Huan Zhou[1], Tao Zhou[2]

1 School of mechanical engineering, Xi'an Jiaotong University, Xi'an, ShanXi, China, **2** Department of college of science, Ningxia medical university, Yinchuan, NingXia, China

* xudan@xjtu.edu.cn

Abstract

In this paper, an adaptive fractional order sliding mode control (AFSMC) scheme is designed for the current tracking control of the Boost-type converter in a Battery/Supercapacitor hybrid energy storage system (HESS). In order to stabilize the current, the adaptation rules based on state-observer and Lyapunov function are being designed. A fractional order sliding surface function is defined based on the tracking current error and adaptive rules. Furthermore, through fractional order analysis, the stability of the fractional order control system is proven, and the value of the fractional order (λ) is being investigated. In addition, the effectiveness of the proposed AFSMC strategy is being verified by numerical simulations. The advantages of good transient response and robustness to uncertainty are being indicated by this design, when compared with a conventional integer order sliding mode control system.

Introduction

Hybrid electric energy storage system (HESS) is an advanced technology of electric vehicles (EV), usually based on the power of battery with an auxiliary device. The auxiliary devices include supercapacitors (SC), flywheels, fuel cells and so on. The SC has high power density, high efficiency, fast charging and a wide range of operating advantages, especially stabilization as an auxiliary power. Because of these good characteristics, Battery/Supercapacitor HESS has gained increasing attention in energy storage community. In the Battery/Supercapacitor HESS, batteries are often used to fulfill the average power demands, whereas SCs are mainly responsible for offering transient high-power delivery. This combination can help alleviate stress on batteries during hard accelerations and regenerative braking in aggressive decelerations [1].

HESS's research involves topology design, battery modeling, supercapacitor modeling and SOC estimation, SOH prediction, DC-DC converter control strategies, power distribution strategies, and system stability analysis [2–5]. We conducted in-depth research on the power management system for electric vehicles, and then proposed a simplified cascading HESS topology configuration with the adaptive sliding mode control algorithm [6–8]. Our research has been applied to SUDA brand electric car successfully. However, excellent HESS system

should also have a high-performance control strategy in addition to just having a reasonable topology.

The control for the HESS primarily focuses on the DC-DC converter. When the EV's power demand is positive, HESS will generally work in the Boost mode, with the battery (after the step-up) together with the supercapacitor to provide power for the load. When the EV needs to recover the braking energy, the HESS works (in the Buck mode) with the supercapacitor (after the step-down) to charge battery. So the control of HESS mainly involves the control of Boost and Buck converter [9]. We studied the fractional terminal sliding mode control algorithm for Buck converter, and achieved good results [10]. However, in the HESS system, the Boost mode is the main mode of operation, while the control strategy of both (HESS/Boost and Buck) modes are significantly different.

In terms of control, the fundamental control frame for a Boost type converter is a challenging work because it is a bi-linear system with a binary input in its exact description, or it can be a saturated linear system in the average model. This Boost type converter is also a minimum phase system with the output to be controlled [11–12].

Sliding mode control (SMC) is one of the effective nonlinear robust control approaches since it keeps the system dynamics controlled in the sliding mode [13]. The sliding mode control (SMC) has many advantages, such as its fast dynamic response, robustness to disturbances, guaranteed stability and simplicity in implementation [14]. There have been a lot of researches on sliding mode control for DC-DC converters. In Ref. [15], Hasan Komurcugil proposed an adaptive terminal sliding mode control strategy for Buck converter, and his sliding surface is a linear one based on linear combination of the system states(with an appropriate time-invariant coefficient). In Ref. [16–17], Wai RJ and his partners researched on in-depth study about the sliding mode control of Boost converter to improve the Boost converter control performance. In Ref. [18–20], the authors pointed out that fractional calculations apply separately to the modeling and control of DC-DC converters, but the discussion was neither specific nor in detail.

Moreover, HESS control pursuits are not only for high precision but also for the battery protection and current stabilization. Unfortunately, the resistance of the battery is not a constant value such that the external input voltage cannot be accurately calculated, and the load variation also cannot be effectively known [21–22]. In Ref. [23], the authors designed a status observer based on the estimates of the load resistor, the external input voltage, the inductor current and the output voltage.

In this paper, we focus on the high-performance control strategy for the Boost mode in the Battery/Supercapacitor HESS, and propose a novel method of adaptive fractional order sliding mode control (AFSMC). Then we utilize this method to design a novel nonlinear fractional order sliding surface function, that is a fusion of the characteristics of adaptive SMC and fractional order calculation (FOC).

The rest of the paper is organized as follows: Section 2 describes the problem statement and system modeling of the Boost mode in Battery/Supercapacitor HESS. Section 3 deals with the design of adaptive control method. Section 4 conducts the design of nonlinear controllers for the Boost mode converter based on the fractional order calculation and the adaptive sliding mode control. Section 5 shows simulation results and compares the AFSMC strategy and ASMC strategy. Finally, our conclusions are drawn in section 6.

Problem statement and system modeling

Fig 1 shows the Equivalent circuit of the Battery/Supercapacitor HESS in Boost mode, where SW is the main switch; D is the output diode; and L,C,R are the input inductor, output
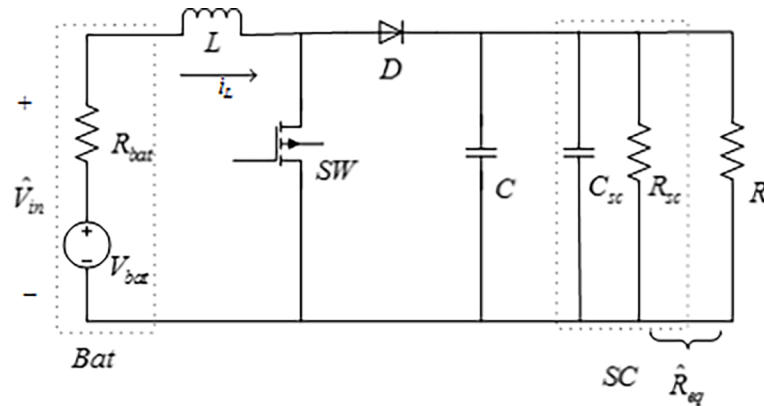
Fig 1. Equivalent circuit of the Battery/Supercapacitor HESS in Boost mode.

capacitor and the load resistor, respectively. The battery is equivalent to power source ($Vbat$) and small resistance ($Rbat$) as input, the supercapacitor is equivalent to capacitance (Csc) and large resistance (Rsc) as output.

By using the state-space averaging method, the average model of this equivalent circuit can be represented as

$$\dot{i}_L = \frac{-(1-u)}{L} V_o + \frac{1}{L} V_{in} \tag{1}$$

$$\dot{V}_o = \frac{(1-u)}{C_{eq}} i_L - \frac{1}{R_{eq} C_{eq}} V_o \tag{2}$$

Where i_L is the average inductor current, V_{in} is the input voltage which can be expressed as $V_{in} = V_{bat} - R_{bat} i_{bat}$, V_{bat} is open circuit voltage of the battery, R_{bat} is the battery resistance, i_{bat} is the battery current, u is the duty-ratio, V_o is the average output voltage.

Selection of the inductor current (i_L) and output voltage (V_o) as state variable of the system:

$$x_1 = i_L \tag{3}$$

$$x_2 = V_o \tag{4}$$

Leads to average state-space model describing the system as the following:

$$\dot{x}_1 = \frac{-(1-u)}{L} x_2 + \frac{1}{L} V_{in} \tag{5}$$

$$\dot{x}_2 = \frac{(1-u)}{C_{eq}} x_1 - \frac{1}{R_{eq} C_{eq}} x_2 \tag{6}$$

Adaptive control and adaptation rules

The control strategy of the equivalent circuit of the Battery/Supercapacitor HESS in Boost mode is similar to the one of the Boost converter. However, the changes of battery resistance and supercapacitor equivalent resistance will cause current and output voltage fluctuations. Unfortunately, the battery resistance and the supercapacitor's resistance are non-linear and dynamic. In order to reduce the magnitude of chattering and guarantee the battery safety, a constant current control for the battery should be implemented. It is necessary to design

adaptive control strategy to overcome the changes in parameters caused by current and voltage fluctuations.

We define the tracking current error and the output voltage error as

$$\tilde{x}_1 = x_1 - \hat{x}_1 \tag{7}$$

$$\tilde{x}_2 = x_2 - \hat{x}_2 \tag{8}$$

Where $\hat{x}_1$ and $\hat{x}_2$ are the estimates of x_1 and x_2 respectively. In general $\hat{x}_2 = V_{ref}$ and $\hat{x}_1 = \frac{V_{ref}^2}{V_{in} R_{eq}}$.

Inductor current and output voltage fluctuations are mainly caused by changes in battery internal resistance and load resistance. So, we choose $\hat{V}_{in}$ and $\hat{R}_{eq}$ as estimation. Establish the observation function as

$$\dot{\hat{x}}_1 = \frac{-(1-u)\hat{x}_2}{L} + \frac{\hat{V}_{in}}{L} + \alpha_1(x_1 - \hat{x}_1) \tag{9}$$

$$\dot{\hat{x}}_2 = \frac{(1-u)\hat{x}_1}{C_{eq}} - \frac{x_2}{\hat{R}_{eq} C_{eq}} + \alpha_2(x_2 - \hat{x}_2) \tag{10}$$

Where α_1 and α_2 are positive integers, used to amplify the estimated value and the actual value of the error.

Define $G_{eq} = \frac{1}{R_{eq}}$, $\tilde{G}_{eq} = G_{eq} - \hat{G}_{eq}$ and $\tilde{V}_{in} = V_{in} - \hat{V}_{in}$, we can obtain

$$\dot{\tilde{x}}_1 = \frac{-(1-u)\tilde{x}_2}{L} + \frac{\tilde{V}_{in}}{L} - \alpha_1 \tilde{x}_1 \tag{11}$$

$$\dot{\tilde{x}}_2 = \frac{(1-u)\tilde{x}_1}{C_{eq}} - \frac{\tilde{G}_{eq} x_2}{C_{eq}} - \alpha_2 \tilde{x}_2 \tag{12}$$

Defining the Lyapunov function as

$$V = \frac{1}{2} L \tilde{x}_1^2 + \frac{1}{2}(C + C_{sc})\tilde{x}_2^2 + \frac{1}{2\beta_1}\tilde{G}_{eq}^2 + \frac{1}{2\beta_2}\tilde{V}_{in}^2 \tag{13}$$

Where β_1 and β_2 are the given positive constants. The time derivative of Eq (13) can be written as

$$\dot{V} = L\tilde{x}_1 \dot{\tilde{x}}_1 + (C + C_{sc})\tilde{x}_2 \dot{\tilde{x}}_2 + \frac{1}{\beta_1}\tilde{G}_{eq}\dot{\tilde{G}}_{eq} + \frac{1}{\beta_2}\tilde{V}_{in}\dot{\tilde{V}}_{in} \tag{14}$$

Substitute (11) and (12), Eq (14) can be represented as

$$\dot{V} = -L\alpha_1 \tilde{x}_1^2 - \alpha_2(C + C_{sc})\tilde{x}_2^2 - \tilde{G}_{eq}\left(x_2 \tilde{x}_2 + \frac{\dot{\hat{G}}_{eq}}{\beta_1}\right) + \tilde{V}_{in}\left(\tilde{x}_1 - \frac{\dot{\hat{V}}_{in}}{\beta_2}\right) \tag{15}$$

To ensure the stability of the system, the adaptation rules are designed as $\dot{\hat{G}}_{eq} = -\beta_1 x_2 \tilde{x}_2$ and $\dot{\hat{V}}_{in} = \beta_2 \tilde{x}_1$. With the adaptation rules, the Eq (15) obtain

$$\dot{V} = -L\alpha_1 \tilde{x}_1^2 - \alpha_2(C + C_{sc})\tilde{x}_2^2 < 0 \tag{16}$$

According to the Lasalle principle, it can be know that

$$\tilde{x}_1 \to 0; \quad \tilde{x}_2 \to 0 \tag{17}$$

In view of Eqs (9) and (10), it can conclude that $\hat{x}_2 \to V_{ref}$, $\hat{V}_{in} \to V_{in}$, $\hat{G}_{eq} \to G_{eq}$ asymptotically.

Fractional order sliding mode control

The sliding surface function is expressed as a fractional order differential equation that is obtained in the form

$$S(t) = \tilde{x}_1 + kD_0^{-\lambda}\tilde{x}_1 \tag{18}$$

Where $\lambda \in [0,1]$, k is positive constant. For the Boost mode with FSMC, the time derivative of Eq (18) can be written as

$$\dot{S}(t) = \frac{-(1-u)\tilde{x}_2}{L} + \frac{\tilde{V}_{in}}{L} - \alpha_1\tilde{x}_1 + kD_0^{-\lambda}\left(\frac{-(1-u)\tilde{x}_2}{L} + \frac{\tilde{V}_{in}}{L} - \alpha_1\tilde{x}_1\right) \tag{19}$$

By setting $\dot{S}(t) = 0$ the equivalent control is obtained, and it has the owing formula:

$$u_{eq} = 1 - \frac{\tilde{V}_{in} - \alpha_1 L\tilde{x}_1}{\tilde{x}_2} \tag{20}$$

Then, the global control is given by:

$$u = 1 - \frac{\tilde{V}_{in} - \alpha_1 L\tilde{x}_1}{\tilde{x}_2} + K \cdot D_0^{-\lambda}(\text{sgn}(S)) \tag{21}$$

Substituting of (21) in (19) results:

$$\dot{S}(t) = -K \cdot D_0^{-\lambda}(\text{sgn}(S(t))) - K \cdot D_0^{-\lambda}(\text{sgn}(S(0))) \tag{22}$$

For initial condition $x_1 = 0$, the sliding surface $S(0) = 0$, then Eq (22) can be rewritten as the following:

$$\dot{S}(t) = -K \cdot D_0^{-\lambda}(\text{sgn}(S(t))) \tag{23}$$

By selecting the Lyapunov function as

$$V = S^2 \tag{24}$$

The time derivative of Eq (24) can be written as

$$\dot{V} = 2S\dot{S} \tag{25}$$

Using Eq (23), then Eq (25) can be obtained as

$$\dot{V} = 2S(t)\dot{S}(t) = -2K \cdot S \cdot D_0^{-\lambda}(\text{sgn}(S)) \leq 0 \tag{26}$$

As can be seen from Eq (26), the proposed sliding surface can satisfy the stability condition.

Furthermore, through the fractional version of Lyapunov by direct method, the same relationship can also be proven [24]. It follows from the Ref. [25], if 0 is the equilibrium point of

Table 1. Specifications of equivalent circuit of the Battery/Supercapacitor HESS in Boost mode.

Descriptions	Parameters	Nominal values
Battery	$Vbat, C$	25V, 55Ah
Supercapacitor	Vsc, Csc	50 V, 15.7F
Desired output voltage	$Vref$	50V
Inductance	L	260 uH
Capacitance	C	100 uF
Load resistance	R	5Ω

system (21) and $x(0) = x_0$, then the fractional order derivative of Eq (24), can be written as

$$D^{1-\lambda}V = D^{-\lambda}\dot{V} \leq -KD^{-\lambda}\|x_1\|$$
$$= -Kl^{-1}D^{-\lambda}\|S\| \leq -Kl^{-1}\|D^{-\lambda}S\| \quad (27)$$
$$= -Kl^{-1}\|x_1\|$$

Where K is positive constant, l is Lipschitz constant and $l > 0$. So, we can find $V > 0$ and $D^{1-\lambda}V < 0$. In other words, the controlled system satisfies the reaching condition.

Simulation and discussion

In order to show the performance of the AFSMC, the equivalent circuit of Boost mode system was subsequently tested by simulations. Simulations are carried out using MATLAB/Simulink. The parameters of equivalent circuit are given in Table 1.

When the supercapacitor's open circuit voltage and SOC are low, we approximate that V_{bat} = 25 V, V_{sc} = 0 V, V_{ref} = 50 V, in this simulation study. Further, we investigated the dynamic response of output voltage with different fractional orders (λ) on the basis of the adaptive fractional order sliding mode control strategy. The control gains of the AFSMC system are given as follows: $\alpha_1 = 6G_{eq}/C$, $\alpha_2 = 2G_{eq}/C$, $\beta_1 = 2$, $\beta_2 = 100$, $k = 300$.

Fig 2 shows the simulated start-up and transient responses of the output voltage obtained by AFSMC strategies with different λ values. It is interesting to note that the output voltage responses become faster with decreasing the value of λ, but when $\lambda = 0.4$, the overshoot of the system appears and exceeds 10%. In order to ensure the safety of SC and obtain high
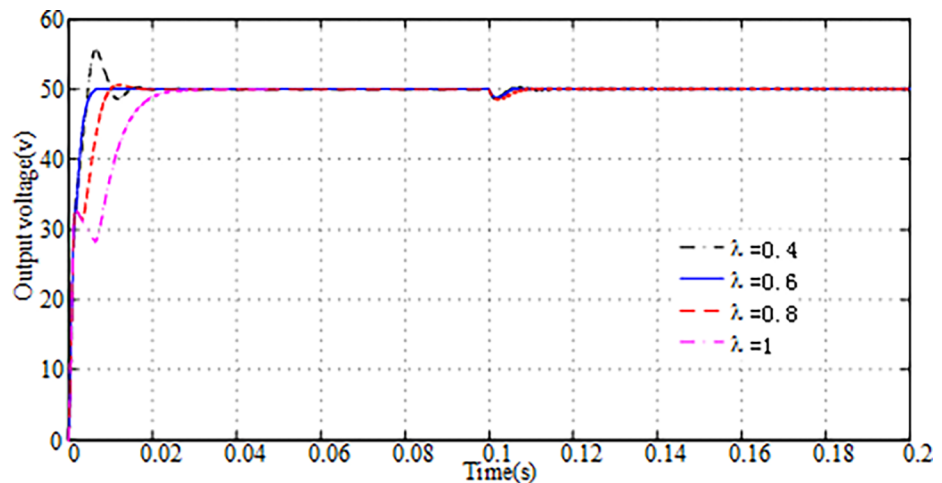

Fig 2. Simulated output voltage responses due to the different λ by AFSMC.
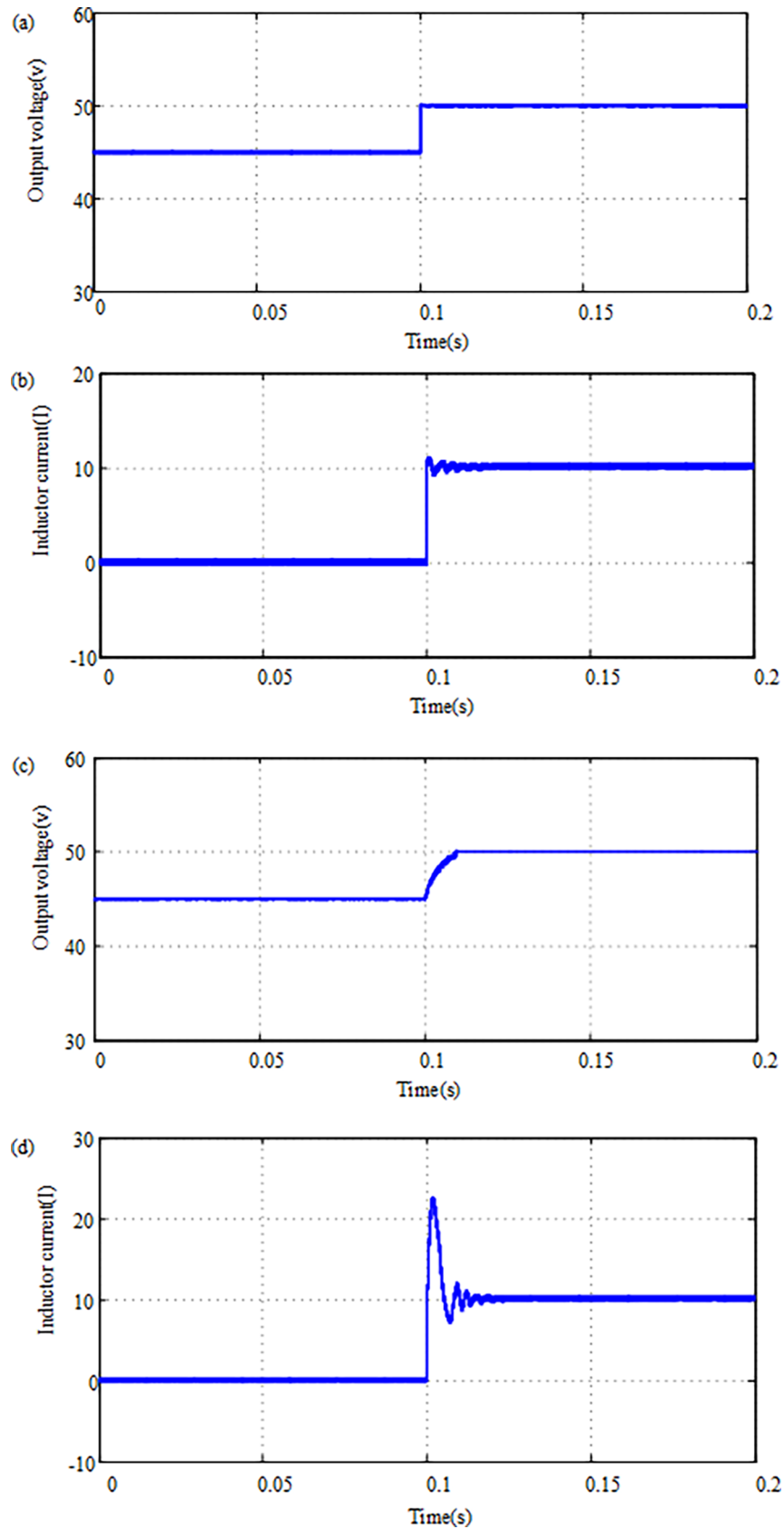
Fig 3. Simulation results of the FASMC and ASMC strategy for the Battery/supercapacitor HESS: (a) The turn-on voltage of the FASMC; (b) The inductor current of the FASMC; (c)The turn-on voltage of the ASMC; (d) The inductor current of the ASMC.

performance control strategy, we should try to avoid the voltage overshoot and chattering. And at $t = 0.1$s, the load resistance is changed from 5Ω to 1 Ω. Therefore, the output current will be increased for this t-value, and the output voltage has a short step-down. It can be seen that the actual output voltage returns faster to desired voltage with decreasing the value of λ, too. So λ = 0.6 is our choice for ideal parameter value.

When the SOC of supercapacitor is high, we approximate that $V_{bat} = 25$ V, $V_{sc} = 45$ V, $V_{ref} = 50$ V simulation study. At $t = 0.1$s, we start the converter and make the output 45V boost to 50V. We investigated and compared AFSMC (λ = 0.6) and ASMC (λ = 1), respectively. The output voltage response and the inductor current at conditions AFSMC and ASMC are shown in Fig 3. From Fig 3(A)–3(D), we can see that both control strategies have in-rush current at start-up, which is caused by the MOS and capacitor. However, the current is significantly more stable in AFSMC strategy. In addition, it can be known that the AFSMC strategy can reduce the adjusting time of the turn-on voltage, as compared with the ASMC strategy. It can improve up to 80% of the transient time during startup of the Boost mode converter.

Conclusions

The application of a AFSMC system to achieve a steady inductor current and control output voltage of the Boost mode in Battery/supercapacitor HESS has been successfully demonstrated. Fristly, the description of the equivalent circuit of the Battery/supercapacitor HESS in Boost mode and system modeling was introduced. Then, the design procedure and the stability analyses of the proposed AFSMC scheme were described in detail. Moreover, numerical simulations in different operational conditions were carried out, and the dynamic response of output voltage with different fractional orders were investigated. According to the simulation results, when the fractional order ($λ$) equals to 0.6, the performance of dynamic responses is better than the other values of λ. Compared with the integer order ASMC strategy, the fractional order ASMC method decreases 10% of the transient time to deal with the load variation. It also reduces 80% of the transient time during the startup of the Boost mode converter. Therefore, the AFSMC strategy not only provides a constant current, but also allows the HESS system to reach a steady state quickly. So, this application of the AFSMC strategy to the HESS of an electric vehicle will improve the overall performance.

Author Contributions

Funding acquisition: Dan Xu, Tao Zhou.

Methodology: Jianlin Wang, Dan Xu.

Resources: Tao Zhou.

Software: Jianlin Wang, Huan Zhou.

References

1. Cao J, Emadi A. A New Bat/UltraCapacitor Hybrid Energy Storage System for Electric, Hybrid, and Plug-In Hybrid Electric Vehicles. IEEE Transactions on Power Electronics. 2011; 27(1):122–132.

2. Hu X, Jiang J, Cao D. Battery Health Prognosis for Electric Vehicles Using Sample Entropy and Sparse Bayesian Predictive Modeling. IEEE Transactions on Industrial Electronics. 2016; 63(4):2645–2656.

3. Wang Z, Ma J, Zhang L. State-of-Health Estimation for Lithium-Ion Batteries Based on the Multi-Island Genetic Algorithm and the Gaussian Process Regression. IEEE Access. 2017; 5:21286–21295.

4. Zhang L, Hu X, Wang Z. A review of supercapacitor modeling, estimation, and applications: A control/management perspective. Renewable & Sustainable Energy Reviews. 2017; 81:1868–1878

5. Zhang L, Hu X, Wang Z. Multi-Objective Optimal Sizing of Hybrid Energy Storage System for Electric Vehicles. IEEE Transactions on Vehicular Technology. 2017: PP (99):1–1.

6. Wang B, Xu J, Cao BG, Zhou X. A novel multimode hybrid energy storage system and its energy management strategy for electric vehicles. Journal of Power Sources. 2015; 281:432–443.

7. Wang B, Xu J, Cao BG. Design of a novel hybrid power for EV. Transportation Electrification Asia-Pacific. IEEE, 2014:1–5.

8. Wang B, Xu J, Cao BG. Compound-Type Hybrid Energy Storage System and Its Mode Control Strategy for Electric Vehicles. Journal of Power Electronics. 2015; 15(3):849–859.

9. Barhoumi S, Sahbani A, Saad K B. Sliding Mode Control for a Boost converter with Constant Power Load. International Conference on Control Engineering & Information Technology. IEEE. 2017:1–5.

10. Wang J, Xu D, Zhou H, Bai A. High-performance fractional order terminal sliding mode control strategy for DC-DC Buck converter. Plos One. 2017; 12(10):e0187152. https://doi.org/10.1371/journal.pone.0187152 PMID: 29084255

11. Ghasemian A, Taheri A. Constrained Near Time-Optimal Sliding Mode Control of Boost Converters Based on Switched Affine Model Analysis. IEEE Transactions on Industrial Electronics. 2017; (99):1–1.

12. Oucheriah S, Guo L. PWM-Based Adaptive Sliding-Mode Control for Boost DC–DC Converters. IEEE Transactions on Industrial Electronics. 2013; 60(8):3291–3294.

13. Silva FA. Sliding mode control of switching power converters: techniques and implementation. IEEE Industrial Electronics Magazine. 2012; 38(2–3): 203–213.

14. Li H, Wang J, Lam HK, Zhou Q, Du H. Adaptive Sliding Mode Control for Interval Type-2 Fuzzy Systems. IEEE Transactions on Systems Man & Cybernetics Systems. 2016; PP(99):1–10.

15. Komurcugil H. Adaptive terminal sliding-mode control strategy for DC-DC Buck converters. Isa Transactions. 2012; 51(6):673–681. https://doi.org/10.1016/j.isatra.2012.07.005 PMID: 22877744

16. Wai RJ, Shih LC. Design of Voltage Tracking Control for DC–DC Boost Converter Via Total Sliding-Mode Technique. IEEE Transactions on Industrial Electronics. 2011; 58(6):2502–2511.

17. Wai RJ, Lin YF, Liu YK. Design of Adaptive Fuzzy-Neural-Network Control for a Single-Stage Boost Inverter. IEEE Transactions on Power Electronics. 2015; 30(12):7282–7298.

18. Delghavi MB, Shoja-Majidabad S, Yazdani A. Fractional-Order Sliding-Mode Control of Islanded Distributed Energy Resource Systems. IEEE Transactions on Sustainable Energy. 2016; 7(4):1482–9.

19. Delavari H, Ghaderi R, Ranjbar A, Momani S. Fuzzy fractional order sliding mode controller for nonlinear systems. Communications in Nonlinear Science & Numerical Simulation. 2010; 15(4):963–15.

20. Bouarr N., Boukhetala D., Benlahbib B., Batoun B. Sliding Mode Control based On Fractional Order Calculus For DC-DC converters. International Journal of Mathematical Modelling & Computations. 2015; 05(04):319–333

21. Zou C, Hu X, Dey S, Zhang L. Nonlinear Fractional-Order Estimator With Guaranteed Robustness and Stability for Lithium-Ion Batteries. IEEE Transactions on Industrial Electronics. 2018; 65(7):5951–5961.

22. Zou C, Hu X, Wei Z, Tang X. Electrothermal dynamics-conscious lithium-ion battery cell-level charging management via state-monitored predictive control. Energy. 2017; 141:250–259.

23. Wang B, Xu J, Yan Z. Duty-ratio based adaptive sliding-mode control method for boost converter in a hybrid energy storage system. The, International Conference on Applied Energy—ICAE. 2016.

24. Wu GC, Baleanu D, Luo WH. Lyapunov functions for Riemann–Liouville-like fractional difference equations. Applied Mathematics & Computation. 2017; 314:228–236.

25. Li Y, Chen YQ, Podlubny I. Stability of fractional-order nonlinear dynamic systems: Lyapunov direct method and generalized Mittag–Leffler stability. Computers & Mathematics with Applications. 2010; 59 (5):1810–1821.